Carbohydrate Polymers 88 (2012) 1425–1434

Contents lists available at SciVerse ScienceDirect

Carbohydrate Polymers

journal homepage: www.elsevier.com/locate/carbpol

Structural characterization and biological properties of degradation byproducts from hyaluronan after acid hydrolysis

Daniela Šmejkalová*, Martina Hermannová, Radovan Buffa, Dagmar Čožíková, Lucie Vištejnová, Zuzana Matulková, Jaroslav Hrabica, Vladimír Velebný

Contipro Pharma, Dolní Dobrouč 401, 561 02 Dolní Dobrouč, Czech Republic

ARTICLE INFO

Article history:
Received 11 January 2012
Received in revised form 6 February 2012
Accepted 13 February 2012
Available online 22 February 2012

Keywords:
Hyaluronan
Degradation products
Acid hydrolysis
NMR
Mass spectrometry

ABSTRACT

The generation of degradation byproducts from hyaluronan during its acid hydrolysis was studied. The degradation byproducts were removed from reaction mixture by ultrafiltration, followed by ionex separation and purification on a reversed-phase HPLC column. Isolated fractions were structurally analyzed by NMR and mass spectrometry. Results indicated that when acid hydrolysis is performed at 100 °C for 24 h, about 0.7% of high molar mass hyaluronan (1.2×10^6 g mol^{-1}) was converted into furan-like derivatives. Other major degradation byproducts present in 0.2 wt% amounts were identified as derivatives of cyclopentanone. Cell viability tests indicated that most of the degradation byproducts have negative effect on cell growth. These tests were performed using mouse fibroblast cell line 3T3 and human keranocytes cell line HaCaT. For this reason, it is important to evaluate the amount of degradation byproducts in low molar mass hyaluronan produced by acid hydrolysis, mainly when these products are used in pharmaceutical and cosmetic applications. During this study it was found out that the unwanted degradation byproducts can be completely removed when an ultrafiltration step is introduced after acid hydrolysis prior hyaluronan isolation.

1. Introduction

Hyaluronan (HA) is a linear polysaccharide consisting of alternating units of D-glucuronic acid and *N*-acetyl-D-glucosamine linked by β(1,3) and β(1,4) linkages. The weight-average molecular weight of synovial hyaluronan has usually been reported in the order of several millions (Laurent & Fraser, 1992; Laurent, Laurent, & Fraser, 1995). HA is ubiquitously distributed in the mammalian extracellular matrix. It is involved in many fundamental biological processes including cellular adhesion, mobility, proliferation, and differentiation.

It is well established that HA functions depend on the chain size of the polymer. For example, HA fragments having molar mass (M_w) of 2.5×10^5 g mol^{-1} induce expression of genes involved in the inflammation process of macrophages (McKee et al., 1997, 1996) and in carcinoma cells (Fitzgerald, Bowie, Skeffington, & O'Neill, 2000), whilst native HA has an anti-inflammatory effect (Delmage, Powars, Jaynes, & Allerton, 1986; Deschrevel, Tranchepain, & Vincent, 2008). Furthermore, HA fragments with reduced M_w are sometimes required due to the different physical and chemical characteristics of this material, such as low viscosity and higher solubility in aqueous solutions (Melander & Tømmeras, 2010).

Manufacturing of low-molar mass (LMM) HA polysaccharides and HA oligosaccharide products often involves acid hydrolysis (Tokita & Okamoto, 1995; Melander and Tømmeras, 2010). Reduction of the M_w is performed when heating the polysaccharide solution in the presence of mineral acid such as HCl and H_2SO_4. Although this process of M_w reduction is inexpensive, fast and reproducible, the major drawback of such chemical process is the possibility of polysaccharide transformation into furan derivatives. In fact, furan-like compounds are well described as the main products of monosaccharide acid hydrolysis (Kroh, 1994; Tong, Ma, & Li, 2010). Furan compounds are known to be carcinogenic and thus they represent unwanted side reaction products during hyaluronan acid hydrolysis. Conversely, furanoic products are considered to be an important replacement of oil-derived chemicals (Boisen et al., 2009; Tong et al., 2010). The derivatives of furfural are particularly suitable for the preparation of polymeric synthetic materials including polyesters, polyamides and polyurethane (Gandini & Belgacem, 1997, 2002; Moreaua, Belgacem, & Gandini, 2004).

Up to our knowledge, there is no publication related to the determination of reaction byproducts of hyaluronan during acid hydrolysis. However, from the facts stated above it is clear that evaluation of such byproducts is necessary in order to eliminate possible negative aspects considering toxicity of LMM hyaluronan or its oligosaccharides due to the presence of furan-like impurities.

* Corresponding author. Tel.: +420 465519569; fax: +420 465543793.
E-mail addresses: smejkalova@contipro.com, daniela.smejkalova@contipro.com (D. Šmejkalová).

0144-8617/$ – see front matter © 2012 Elsevier Ltd. All rights reserved.
doi:10.1016/j.carbpol.2012.02.031

The aim of this work was to perform hyaluronan acid hydrolysis to oligosaccharides, isolate all degradation byproducts except for oligosaccharides from the reaction mixture, fractionate them, and evaluate their structure and their biological properties regarding cytotoxicity.

2. Materials and methods

2.1. Materials

Hyaluronic acid sodium salt was provided by Contipro Biotech, Czech Republic. Ethylacetate, HCOOH, methanol, NaOH, NaCl, H_2SO_4, 4-hydroxy-5-methyl-3-furanone, 5-(hydroxymethyl)furfural, 2-furoic acid and deuterated water were of analytical grade and purchased from Sigma–Aldrich.

2.2. Hyaluronan degradation

HA (45 g, $M_w = 1.2 \times 10^6$ g mol^{-1}) was dissolved overnight in 4500 mL of demineralized water under constant stirring. The pH was adjusted to pH 3 by 5% H_2SO_4. The acidified solution was transferred into a flask equipped with a condenser and a stirrer, and was heated at 100 °C for 24 h. After this time, the degraded HA solution was cooled in an ice bath, and pH was adjusted to pH 6.5 with 5% NaOH. Then four different procedures including ultrafiltration, dialysis, extraction and ionex separation were applied in order to isolate degradation byproducts from the reaction mixture containing also HA oligomers. The isolation procedures are described below.

2.3. Isolation of degradation byproducts (DB)

Ultrafiltration. The reaction mixture was ultrafiltred through 2 kDa membrane using Hydrosart® ultrafiltration cassette (Sartorius Stedim Biotech GmbH) while collecting permeate. The ultrafiltration was stopped when colorless permeate was observed. Prior HPLC analyses, the collected permeate was concentrated by evaporation (waterbath $T = 39$ °C).

Dialysis. The reaction mixture was evaporated to about 1/10 of the original volume. This concentrate was dialyzed (dialysis Tubing, Avg. flat width 32 mm (1.27 in.), Sigma–Aldrich) against distilled water for two days. Both permeate and retentate were concentrated by evaporation (waterbath $T = 39$ °C) and analyzed by HPLC.

Extraction. The reaction mixture was saturated with NaCl, and three times extracted with ethylacetate. The organic phase was concentrated by evaporation (waterbath $T = 25$ °C) and analyzed by HPLC.

Ionex separation. The reaction mixture was ultrafiltred through 2 kDa membrane using Hydrosart® ultrafiltration cassette (Sartorius Stedim Biotech GmbH) while collecting permeate. Permeate was concentrated by evaporation and separated on a glass column (450 mm × 50 mm, Pall Corporation) filled with AG®1-X8 Resin (Bio-Rad Laboratories) at ambient temperature. An Alliance HPLC system (2695 Separation Module, Waters) equipped with 2998 Photodiode Array (PDA) Detector (Waters) was used for the separation. The chromatographic eluent consisted of a binary phase made from water (A) and 1 M sodium chloride (B) and was pumped at a constant flow-rate of 10 mL min^{-1}. The following gradient was used for the separation: B was held for 60 min at 0%, increased to 5% over 1 min, held at 5% for 260 min, increased to 100% over 4 min, held at 100% for 315 min, and finally decreased to 0% over 5 min. Each 200 mL of eluate (i.e. 20 min of chromatographic run) from 150 to 270 min was collected manually as separate fraction into a glass beaker, concentrated by means of evaporation and purified on a reversed-phase HPLC column. Chromatographic conditions for purification are described below (HPLC analysis of DB).

2.4. HPLC analysis and purification of DB

Two Shimadzu LC-20 AD pumps equipped with SIL-20 A autosampler were used for the analysis of isolated DB through a semi preparative C18 Jupiter column (250 mm × 10 mm, 4 μm, Proteo 90A) held at constant temperature 30 °C. DAD detector (SPD-M 20A) set at 254 and 280 nm was used to detect the reaction products. Data were collected using the LC solution software. The chromatographic eluent consisted of a binary phase made of 0.1% formic acid in water (A) and 0.1% formic acid in acetonitrile (B) that was pumped at 3.0 mL min^{-1} with the following gradient mode: B was held for 10 min at 0%, increased to 4% over 20 min, increased to 10% over 10 min, increased to 30% over 10 min, increased to 100% over 10 min, and finally held at 100% for 10 min. Reaction byproducts were automatically collected using fraction collector FRC-10A at following intervals: (A) 21.25–23.00 min, (B) 25.35–25.80 min, (C) 26.20–26.90 min, (D) 33.55–34.40 min, (E) 40.00–41.25 min repeatedly for 20 chromatographic runs into 30 mL pyrex tubes and cumulatively concentrated by means of evaporation. The final yields of fractions A–E were: (A) 55.3 mg, (B) 16.5 mg, (C) 91.6 mg, (D) 87.4 mg, and (E) 108.1 mg. The dried fractions were directly analyzed by NMR spectroscopy and mass spectrometry.

2.5. NMR spectroscopy

Solution-state NMR spectroscopy was carried out on a Bruker Avance III 500 MHz instrument operating at a proton frequency of 500.25 MHz and a carbon frequency of 125.80 MHz. The spectrometer was equipped with a 5 mm Bruker BBFO plus broadband probe with an actively shielded *z*-gradient coil. All of the spectra were acquired and elaborated by Bruker 2.1 Topspin software.

Dried HPLC fractions were dissolved in 0.75 mL of deuterated water and transferred into 5 mm NMR quartz tubes. ^{13}C NMR was acquired applying power gated decoupling pulse sequence, 65536 data points and 5000 scans. CH_3 and CH signals were distinguished from those of CH_2 and quaternary C in DEPT135 pulse sequence. 2D correlation spectroscopy (COSY) NMR experiments were acquired with 16:12:40 gradient ratio (duration, 1 ms), 16 scans, 4096 points in F2 and 128 points in F1. COSY spectra were transformed with a sine-bell weighting function in both dimensions applying a sine-bell shift (SSB) of 0. 2D total correlation spectroscopy (TOCSY) spectra were acquired with a spin-lock period of 80 ms, 16:12:40 gradient ratio (duration 1ms), 16 scans, 4096 points in F2 and 128 points in F1 with 16 scans. The spectra were transformed with a sine-bell weighting function in both dimensions with a SSB value of 0. 2D heteronuclear single quantum coherence (HSQC) heterocorrelated experiments were acquired using a pulse field gradient sequence with 80:20.1:11:−5 gradient ratio (duration, 1 ms), heteroscalar coupling of 145 Hz, 2212 × 256 points in F2 and F1, respectively, and 48 scans. Data were multiplied by squared sine functions in both dimensions with a SSB value of 2. 2D heteronuclear multi bond correlation (HMBC) heterocorrelated experiments were acquired using heteroscalar coupling of 145 and 8 Hz for short and long range coupling, respectively, 4096 × 256 points in F2 and F1, respectively, and 80 scans. Data were multiplied by squared sine functions in both dimensions with a SSB value of 0. 2D diffusion ordered spectroscopy was performed using a bipolar gradient pulse sequence (ledbpgp). Scans (24) were collected using a 2.3 ms sine-shaped pulse (4.6 ms bipolar pulse pair) ranging from 0.674 to 32.030 G cm^{-1} in 24 increments with a diffusion time of 80 ms and 16384 time domain data points. Apodization was made by multiplying data with an exponential function with a line broadening of 0.2 Hz.

2.6. Mass spectrometry

An Acquity UPLC chromatographic system equipped with UV detector and Synapt HDMS mass spectrometer (Waters) was used for the analysis of degradation byproducts. UV signals were simultaneously measured at 280 and 254 nm. The analysis of DB was performed on a C18 Jupiter column (250 mm × 4.6 mm, 4 μm, Proteo 90A) at ambient temperature. The chromatographic eluent consisted of a binary phase of 0.1% formic acid in water (A) and methanol (B) that was pumped at 0.5 mL min^{-1} with the following gradient mode: B was held for 5 min at 0%, increased to 30% over 20 min, increased to 100% over 15 min, held at 100% for 3 min, decreased on 0% over 7 min, and held at 0% over 5 min.

The mass spectrometer was equipped with an electrospray ionization source operating in both negative and positive ion mode. The effluent was introduced into an electrospray source with an UPLC pump directly after the column separation. Nitrogen was used as cone gas (50 L/h) and desolvation gas (500 L/h). Capillary voltage was set at 2.7 kV. Sampling cone was set at 20 V. Extraction cone was set at 5. The source block temperature was set at 100 °C, while the desolvation temperature was 250 °C. For each sample full MS scan from *m/z* 50 to 1000 was acquired. For MS/MS, argon was used as a collision gas. The collision energy ramp from 5 eV up to 25 eV was used to fragment the ion of interest. Data were collected at 1 scan/s and elaborated using the MassLynx software.

2.7. Cell viability assay

Spontaneously immortalized human keratinocyte cell line HaCaT (a kind gift from Prof. Dr. N. Fusenig, Deutsches Krebsforschungszentrum, Heidelberg, Germany) was grown in Dulbecco's modified Eagle's medium-low glucose (DMEM) (Sigma–Aldrich, USA) supplemented with 10% fetal bovine serum (FBS) (Invitrogen, USA), glutamine (0.3 mg ml^{-1}) (Sigma–Aldrich) and gentamicin (50 μg ml^{-1}) (Invitrogen) in 5.0% CO_2 at 37 °C in 75 cm^2 culture flask (TPP, Switzerland). Swiss albino mouse fibroblasts 3T3 (Deutsche Sammlung von Mikroorganismen und Zellkulturen, Germany, DSMZ No. ACC 173) were grown in DMEM supplemented with 10% FBS, glutamine (0.3 mg ml^{-1}), penicillin (100 U ml^{-1}) (Sigma–Aldrich) and streptomycin (0.1 mg ml^{-1}) (Sigma–Aldrich) in 5.0% CO_2 at 37 °C in 75 cm^2 culture flask as recommended by the supplier. 3T3 and HaCaT cell lines were seeded on 96-well test plates at density of 3000 and 4000 cells/well, respectively, and let adhere overnight. Next day, cells were treated by DB at concentration range 100–1000 μg ml^{-1} in full culture medium. The cell viability was determinated by MTT assay described previously (Vistejnova et al., 2009). Briefly, 20 μl of MTT work solution (5 mg ml^{-1}) was added to each well and incubated at 37 °C, 7.5% CO_2 for 2 h. The medium was removed and the cells were lysed in 220 μl of lysis solution (isopropylalcohol: DMSO 1:1, Triton-X, HCl) for 30 min. The optical density was measured every 24 h till 72 h at 570 nm using a Versa Max Microplate Reader (Molecular Devices, Sunnyvale, CA, USA) and corrected by the 690 nm reference wavelength. Results are expressed by relative cell viability, which was calculated as ratio of optical density at 24, 48 and 72 h time points and optical density at 0 h time point. Data are presented as mean ± standard error of the mean (S.E.M.). The statistical significance of obtained data was evaluated by one-way ANOVA followed by Fisher's least significant difference post hoc test. A p-value < 0.05 (*) was considered as statistically significant. All statistical analyses were carried out with Statistica 9.1 (StatSoft, USA).

3. Results and discussion

3.1. Isolation of degradation byproducts from oligomer mixture

Native HA hydrolysis experiments were performed while heating 1% HA solution at pH = 3 for 24 h. This time was found to be sufficient in order to obtain both oligomer HA fragments and colored degradation byproducts (DB), where the major DB, labeled A–E, are shown in Fig. 1a. Since it was observed that HA oligomers were coeluting from C18 column at the same retention time as fractions A–E, it was first necessary to purify the DB from HA oligomers prior their further analysis, mainly because structural elucidation and biological testing of DB could be distorted by the presence of HA oligomers.

A number of techniques including extraction, dialysis, ultrafiltration, and anion-exchange separation were applied for the purpose of removing HA oligomers present in the reaction mixture after acid hydrolysis. While the presence of DB was evaluated on C18 reversed-phase column a complementary HPLC analysis using NH_2-stationary phase was performed in order to detect present oligomers (Fig. 1a–e and f–j, respectively).

The HPLC data in Fig. 1 indicated that none of the procedures led to a complete separation of all five DB (A–E) from HA oligomers. Although a complete removal of HA oligomers was achieved by ethyl acetate extraction (Fig. 1g), only DB C and D were separated (Fig. 1b). DB D was also missing during dialysis (Fig. 1c). The only procedure after which initial concentration of HA oligomers was reduced but at the same time all of the DB were detected was ultrafiltration. In this case, the major portion of HA oligomers was kept in ultrafiltration retentate (Fig. 1j), while the DB A–E with remaining HA oligomers were separated into ultrafiltration permeate (Fig. 1d and h). For this reason, ultrafiltration permeate was used for further purification. The remaining HA oligomers were completely removed applying ionex chromatography and DB A–E were then fractionated and concentrated on a reversed-phase HPLC column in sufficient amount for structural and biological testing.

3.2. Fraction A

Structural elucidation. Fraction A was the earliest eluting compound (t_R = 22.3 min) and thus it was the most polar byproduct among all the fractionated DB. ESI–MS analyses indicated that this compound had a molecular ion of $[M-H]^-$ = 184 with corresponding elemental composition of $C_8H_{11}O_4N_1$. ESI–MS/MS spectrum showed a loss of H_2O and CH_2CO groups suggesting that this compound is hydroxylated as well as acylated (Fig. 2).

^{1}H NMR analysis of fraction A indicated the presence of 6 protons that were unexchangable with deuterated water in 5 sets of proton signals: a singlet at 6.40 ppm (1H), a doublet at 4.83 ppm (1H, J = 2.4 Hz), two doublet of doublets at 3.90 and 3.85 ppm (2H, J = 11.3/4.3 and 11.7/3.7 Hz, respectively), a multiplet at 2.48 ppm (1H) and a singlet at 2.20 ppm (1H). TOCSY NMR spectra revealed the presence of only 1 spin system, involving signals at 4.8–3.90–3.85–2.48 ppm, while COSY cross peaks indicated the coupling between signals resonating at 4.83 and 2.48 ppm, and between 3.90 + 3.85 ppm and 2.48 ppm. Thus H resonating at 2.48 ppm is neighboring with both signals appearing at 4.80 and 3.90 + 3.85 ppm, but the latter signals are not positioned next to each other within the structure of the analyzed compound. ^{13}C NMR spectrum confirmed the presence of 8 carbons, previously suggested from MS analyses. Application of DEPT pulse sequence indicated the presence of one CH_3 group, three CH groups, one CH_2 group and three quaternary carbons. The attribution of carbons and protons was made by a combination of HSQC (showing ^1J cross peaks) and HMBC spectra (detecting ^2J and ^3J correlations). Fraction

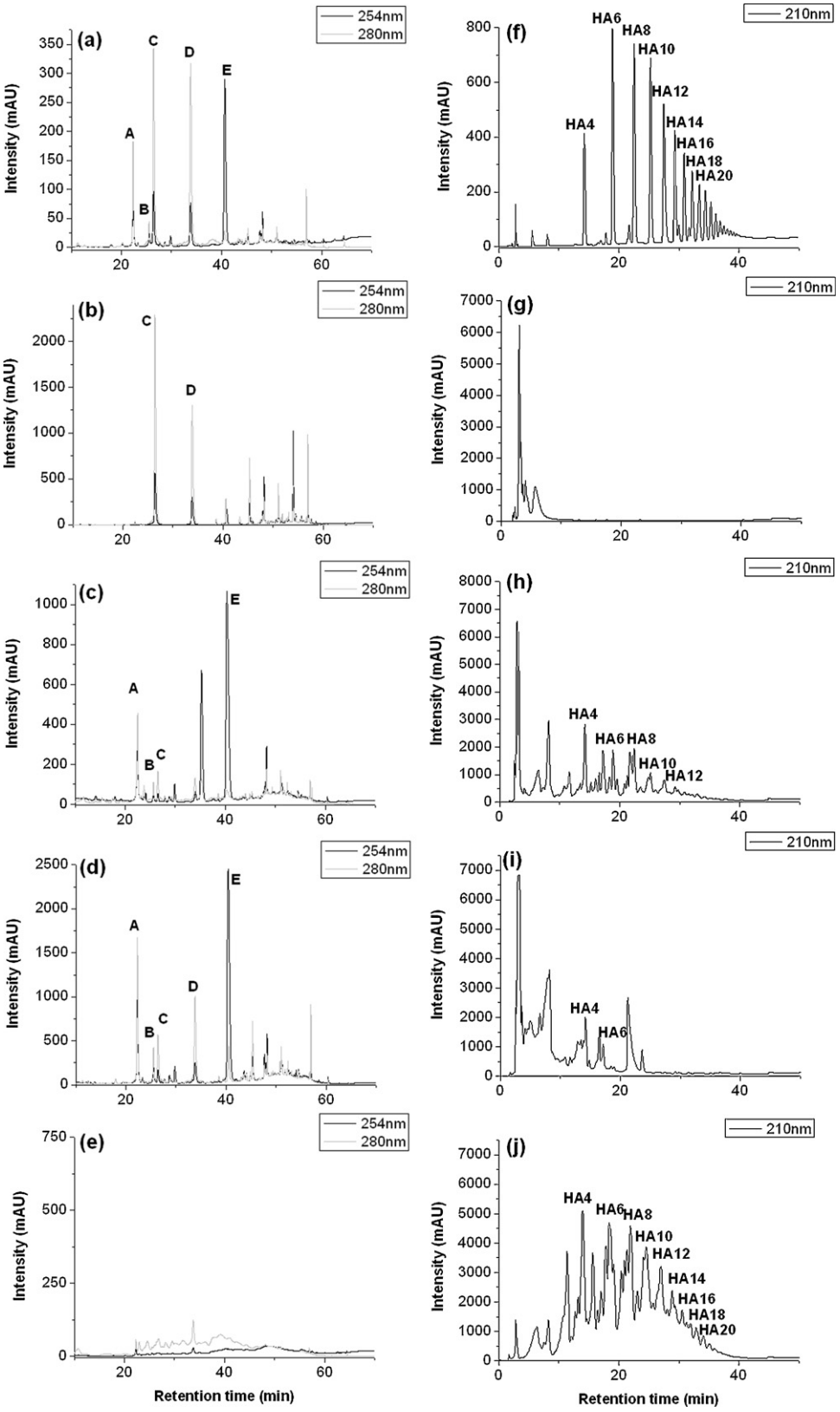

Fig. 1. UV detected degradation byproducts (on the left, a–e) and accompanying HA oligomers (f–j) prepared by hyaluronan acid hydrolysis, where (a and f) are control chromatograms, (b and g) chromatograms after ethylacetate extraction (c and h) after dialysis through 1 kDa membrane-permeate, (d and i) after ultrafiltration through 2 kDa membrane-permeate, (e and j) after ultrafiltration through 2 kDa membrane-retentate.

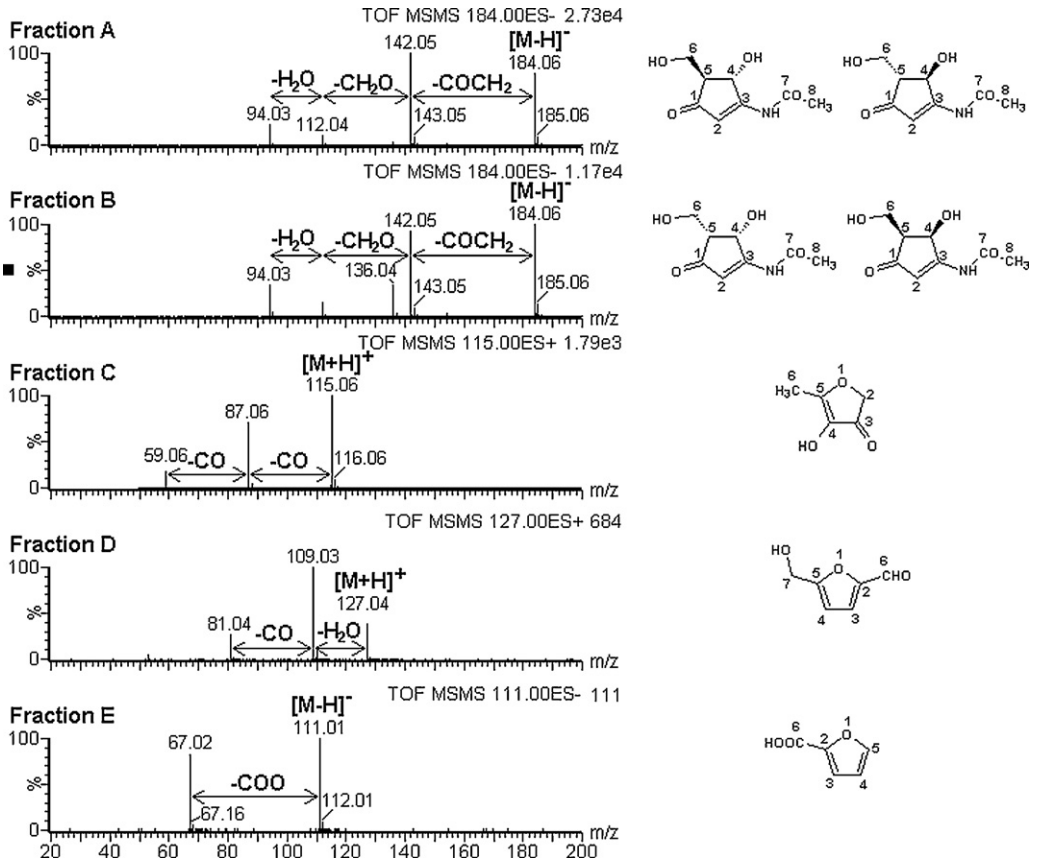

Fig. 2. ESI–MS/MS spectra of fractions (A)–(E), and structures of identified degradation byproducts: (A) ((4*R*,5*S*)- and (4*S*,5*R*)-4-hydroxyl-6-hydroxymethyl-3-*N*-acetamido-cyclopent-2-en-1-one), (B) ((4*R*,5*R*)- and (4*S*,5*S*)-4-hydroxyl-6-hydroxymethyl-3-*N*-acetamido-cyclopent-2-en-1-one), (C) (4-hydroxy-5-methyl-3-furanone), (D) (5-(hydroxymethyl)furfural) and (E) (2-furoic acid).

A was assigned to 4-hydroxyl-6-hydroxymethyl-3-*N*-acetamido-cyclopent-2-en-1-one. Full assignment is given in Table 1 while resulting structure is indicated in Fig. 2 (structure A). The explanation for the shown isomeric (4*R*,5*S*), and (4*S*,5*R*) structure is given later. The identification of fraction A as a derivative of cyclopent-en-one is in agreement with previous findings of Kroh, 1994.

Biological testing. Fraction A was found to have no effect on viability of 3T3 and HaCaT cell lines (Fig. 3).

3.3. Fraction B

Structural elucidation. Surprisingly, fraction B eluting at 25.5 min gave similar mass fragmentation pattern to fraction A (Fig. 2). Since 4-hydroxyl-6-hydroxymethyl-3-*N*-acetamido-cyclopent-2-en-1-one (structures A and B in Fig. 2) has two asymmetric carbons at position 4 and 5, *R* and *S* isomerisation on both chiral centers may occur. Thus 4-hydroxyl-6-hydroxymethyl-3-*N*-acetamido-cyclopent-2-en-1-one may be present in a form of (4*R*,5*S*), (4*S*,5*R*), (4*R*,5*R*) and (4*S*,5*S*) isomers. In fact, the small differences in intensities of mass fragments (Fig. 2) and hardly any chemical shift changes in ^{1}H NMR spectra (Table 1) confirm fraction B to be a structural isomer of fraction A. The only significant difference found during NMR analyses involved a larger magnitude of proton vicinal coupling (J = 6.2 Hz, Table 1) for a doublet corresponding to CH group in position 4 on cyclopent-2-en-1-one ring (B in Fig. 4). This larger vicinal coupling indicated that the dihedral angle between H4 and H5 in fraction B had to be either more eclipsed or antiperiplanar as compared to fraction A (Lambert & Mazzola, 2003). For this reason, fraction B was assigned as a diastereomer consisting of a mixture of enantiomers (4*R*,5*R*) and (4*S*,5*S*), while fraction A was assigned to (4*R*,5*S*), (4*S*,5*R*) diastereomer. This finding is further supported by a strong NOESY cross peak (data not shown) that was detectable between H4 and H6 in fraction A, but was not observed for the same protons in fraction B. The isolation of diastereomers in two different HPLC fractions containing racemic mixtures is in agreement with the fact that separation of enantiomers on a reversed phase column generally does not occur (Kakumanu, Arora, & Bansal, 2006) and chiral column is mostly required for such purpose.

Biological testing. Similarly to fraction A, fraction B was found to have no effect on viability of 3T3 and HaCaT cell lines (Fig. 3).

Generation of DB A and B. Fig. 4 depicts a possible degradation pathway yielding 4-hydroxyl-6-hydroxymethyl-3-*N*-acetamido-cyclopent-2-en-1-one structurally elucidated for fractions A and B. The degradation principally proceeds via aldol-type condensation of double dehydrated open form of *N*-acetyl-D-glucosamine. The intramolecular connection between carbon 1 and 5 is supported by the hydroxyl group in position 4, which causes the nucleophilicity of —C=C— double-bonded carbon in position 5.

3.4. Fraction C

Structural elucidation. Fraction C eluting at 26.5 min had a molecular ion of $[M+H]^+$ = 115 with corresponding elemental composition of $C_5H_6O_3$. ESI–MS/MS spectrum (Fig. 2) showed a double loss of CO group, suggesting fraction C to be a ketone or an aldehyde.

^{1}H NMR analysis of this compound detected 2 singlets, one resonating at 2.22 ppm (3H) and another one at 4.62 (2H). Since the compound was analyzed in D_2O, only one proton was exchangeable and can be attributed to OH or COOH group. ^{13}C NMR spectrum

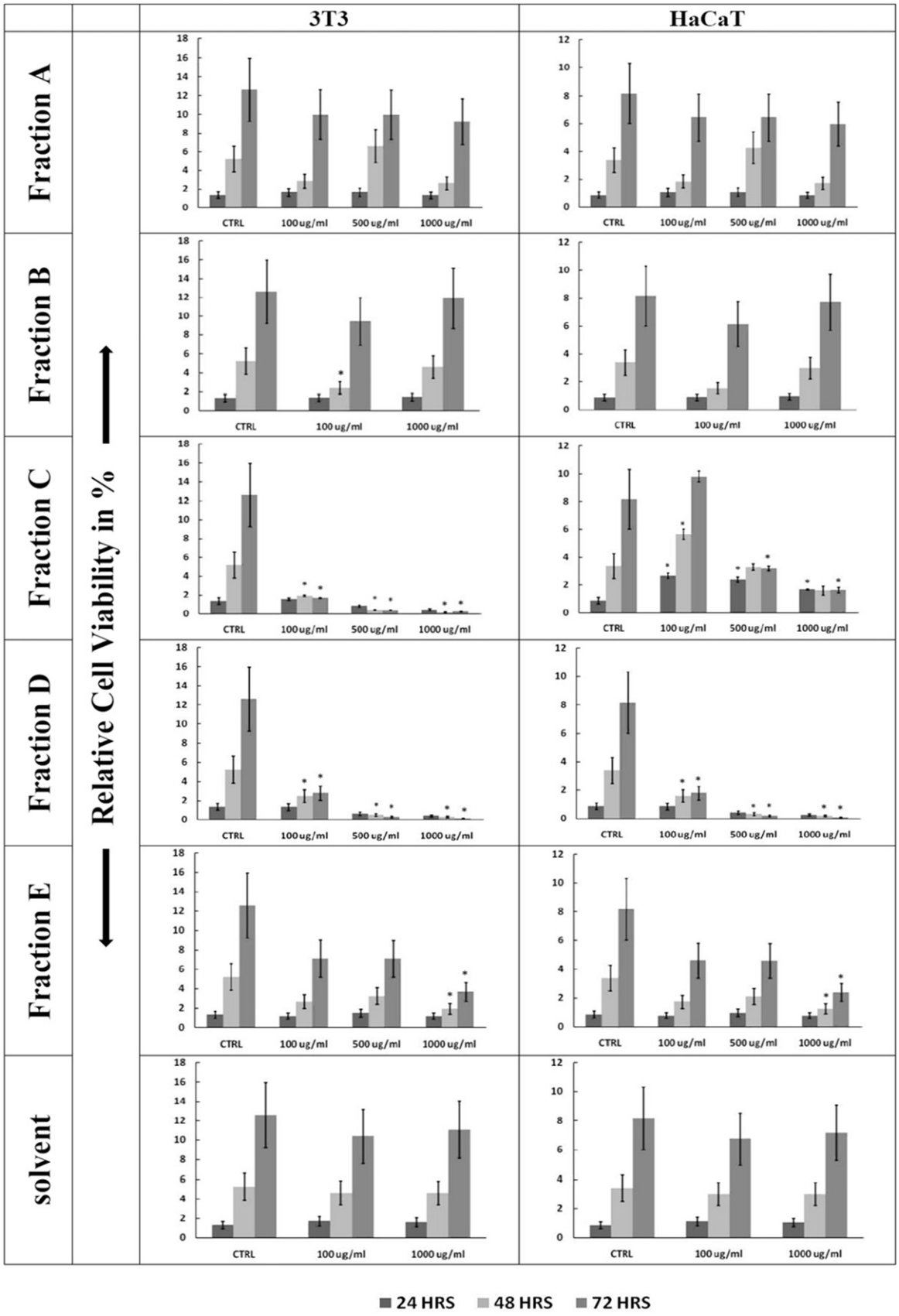

Fig. 3. Effects of fractions A–E and the solvent on cell viability. Mouse fibroblast cell line 3T3 (A) and human keratinocyte cell line HaCaT (B) were treated by fractions A–E and by solvent at concentration 100–1000 $\mu g\,ml^{-1}$ for 72 h. Results are expressed by relative cell viability, which was calculated as ratio of optical density at 24, 48 and 72 h time points and optical density at 0 h time point. Data are presented as mean ± standard error of the mean (S.E.M.). Differences meeting p-value < 0.05 (*) compared to untreated control were considered as statistically significant.

Table 1
^{1}H and ^{13}C chemical shifts (δ) and diffusion coefficients (D) for D_2O solutions of fractionated degradation byproducts A–E formed during acid hydrolysis of hyaluronan. ND stands for not detected.

Position in structure	δ (^{1}H, ppm)	Multiplicity	J (Hz)	δ (^{13}C, ppm)	$D \times 10^{-10}$ ($m^2\ s^{-1}$)
Fraction A					
1	ND	ND	ND	208.0	ND
2	6.40	s	ND	113.2	5.11
3	ND	ND	ND	167.8	ND
4	4.83	d	2.4	71.4	5.15
5	2.48	m	ND	55.3	5.12
6	3.90, 3.85	dd,dd	11.3/4.3, 11.7/3.7	58.1	5.12
7	ND	ND	ND	174.2	ND
8	2.20	s	ND	23.6	5.13
Fraction B					
1	ND	ND	ND	209.0	5.28
2	6.44	s	ND	113.8	ND
3	ND	ND	ND	168.6	ND
4	5.03	d	6.2	70.0	5.28
5	2.75	td	6.0/4.1	50.2	5.28
6	3.89, 3.85	dd, dd	11.6/5.7, 11.3/4.2	28.4	ND
7	ND	ND	ND	174.2	ND
8	2.20	s	ND	23.4	5.27
Fraction C					
2	4.62	s	ND	73.8	6.80
3	ND	ND	ND	198.5	ND
4	ND	ND	ND	180.7	ND
5	ND	ND	ND	133.5	ND
6	2.22	s	ND	12.9	6.80
Fraction D					
2	ND	ND	ND	152.2	ND
3	7.46	d	3.8	127.3	7.14
4	6.61	d	3.8	111.3	7.15
5	ND	ND	ND	161.8	ND
6	9.39	s	ND	180.7	7.12
7	4.63	s	ND	56.3	7.08
Fraction E					
2	ND	ND		144.5	ND
3	7.24	dd	3.6/0.7	118.8	6.94
4	6.68	dd	1.8/0.7	112.3	6.96
5	7.67	dd	3.6/1.8	147.4	6.95
6	ND	ND		162.5	ND

confirmed the presence of 5 carbons, previously suggested from MS analyses. Application of DEPT pulse sequence indicated the presence of one CH_3 group, one CH_2 groups, and three quaternary carbons. Complete attribution of carbons and protons was made by a combination of HSQC (showing ^{1}J cross peaks) and HMBC spectra (detecting ^{2}J and ^{3}J correlations). Fraction C was assigned to 4-hydroxyl-5-methyl-3-furanone. Full assignment is given in Table 1 while resulting structure is indicated in Fig. 2 (structure C). Correctness of the assignment was checked acquiring spectra of a reference standard.

Biological testing. Unlike fractions A and B, fraction C was found to totally decrease 3T3 cell line viability. The viability of HaCaT cell lines was negatively affected by fraction C from concentration 500 $\mu g\ ml^{-1}$ (Fig. 3).

Generation of DB C. As depicted in Fig. 5, the key step in degradation is probably the decarboxylation of glucuronic acid in α,β-unsaturated stage, followed by enol-keto tautomerism and dehydration yielding 3,4-dihydroxy-2-methylfurane, which exists predominantly as mono-keto form 4-hydroxyl-5-methyl-3-furanone.

3.5. Fraction D

Structural elucidation. Fraction D eluted at 33.8 min had a molecular ion of $[M+H]^+ = 127$ with corresponding elemental composition of $C_6H_6O_3$. ESI–MS/MS spectrum (Fig. 2) showed a loss of CO and OH groups suggesting that this compound is an aldehyde/ketone and is hydroxylated.

^{1}H NMR analysis of this compound indicated the presence of 5 unexchangable protons with D_2O in 4 sets of proton signals: a singlet at 9.39 ppm (1H), a doublet at 7.46 ppm (1H, $J = 3.8$ Hz), another doublet at 6.61 ppm (1H, $J = 3.8$ Hz), and another singlet at 4.63 ppm (2H). The low field signal detected at 9.39 ppm can be attributed to CHO group previously identified from mass fragmentation. The detected vicinal coupling of 3.8 Hz is typical for furan-type compounds (Lambert & Mazzola, 2003). The TOCSY crosspeaks indicated that only signals resonating at 7.46 and 6.61 ppm are involved in a spin system. ^{13}C NMR experiment together with DEPT pulse sequence indicated the presence of 2 quaternary carbons at 161.8 and 152.2 ppm, three CH groups at 180.7, 127.3, and 111.3 ppm and one CH_2 functional group resonating at 56.3 ppm. Thus, fraction D was assigned as 5-(hydroxymethyl)furfural (structure D in Fig. 2) and the assignment was checked acquiring spectra of a reference standard.

Biological testing. Fraction D caused entire drop off of cell viability of both 3T3 and HaCaT cell lines (Fig. 3).

Generation of DB D. Fig. 6 depicts a possible degradation pathway yielding 5-(hydroxymethyl)furfural. The key step in this degradation pathway is enolisation of α,β-unsaturated aldehyde which in turn gives rise to α-imino aldehyde. This reactive intermediate can further either undergo hydrolysis of imine group to form α-keto aldehyde followed by cyclisation and double-dehydration, or it can be firstly cyclised by addition reaction of the hydroxyl group to

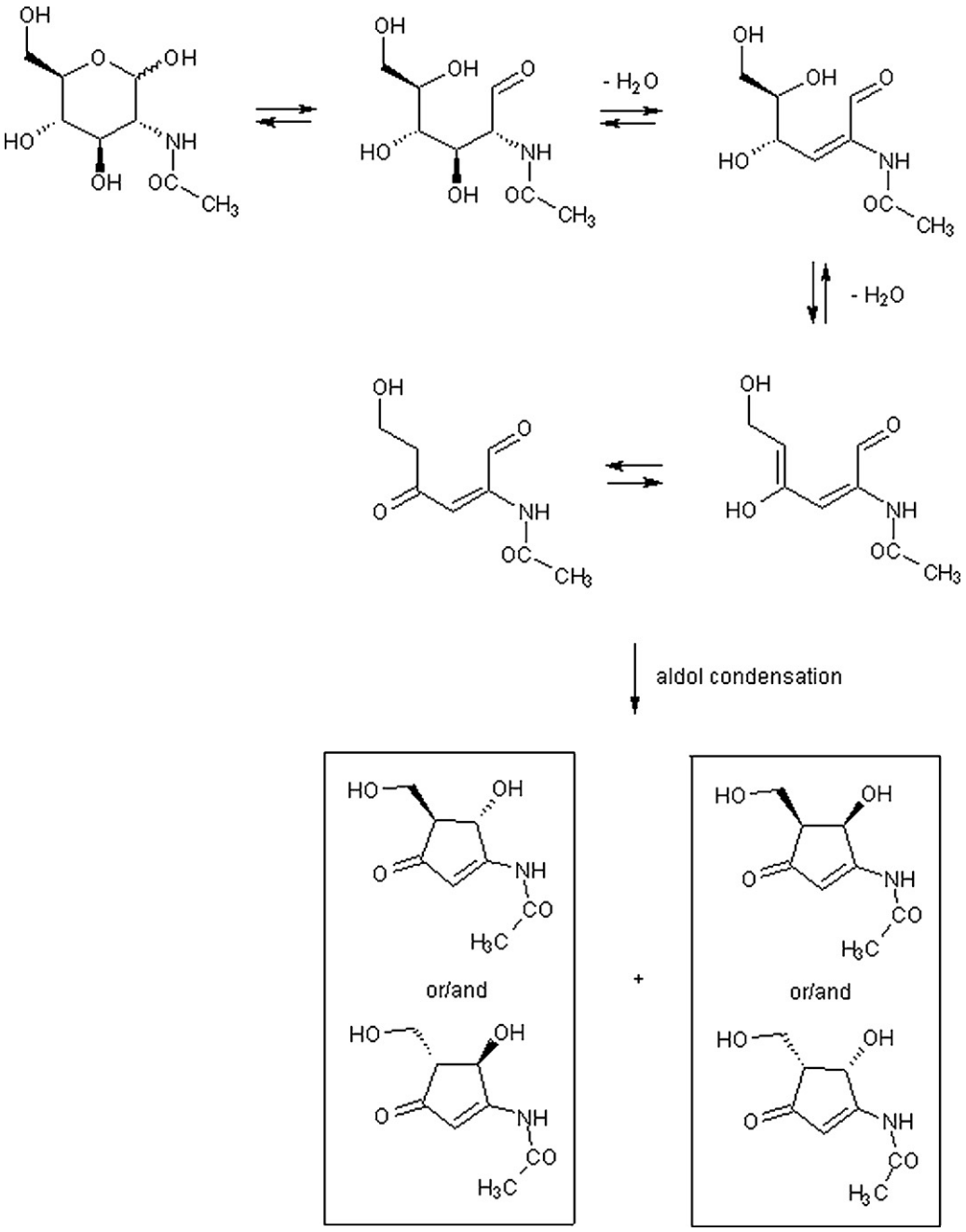

Fig. 4. Possible way of formation of 4-hydroxyl-6-hydroxymethyl-3-*N*-acetamido-cyclopent-2-en-1-one formation during acid hydrolysis of hyaluronan.

the imino carbon followed by elimination of water and acetamide while yielding a stable aromatic system.

3.6. Fraction E

Structural elucidation. Fraction E was the last eluting compound (t_R = 40.4 min) and thus it was the least polar compound among all the fractionated DB. ESI–MS analyses indicated that this compound had a molecular ion of $[M-H]^-$ = 111, corresponding to elemental composition of $C_5H_4O_3$. ESI–MS/MS spectrum showed a loss of 44 typical for fragmentation of COO groups suggesting that this compound is probably a carboxylic acid (Fig. 2).

Three sets of doublet of doublets were detected in ^{1}H NMR spectra: the first one was resonating at 7.67 ppm (1H, J = 1.8/0.7 Hz), second at 7.24 ppm (1H, J = 3.6/0.7 Hz), and third at 6. 58 ppm (1H, J = 3.6/1.8 Hz). The observed J coupling indicated that all detected protons are part of one spin system. Moreover, the J magnitude is typical for furans substituted in position 2 on the ring (Lambert & Mazzola, 2003). Thus fraction E was assigned as 2-furoic acid (E in Fig. 2). The correctness of this assignment was further checked by ^{13}C NMR analysis where two quaternary C and three CH functional groups were detected and by comparison to a reference standard spectrum.

Biological testing. Fraction E was found to affect negatively 3T3 and HaCaT cell lines only at concentrations higher than 1000 μg ml^{-1} (Fig. 3).

Generation of DB E. Fig. 7 depicts a thermal degradation pathway of D-glucuronic acid that proceeds via dicarbonyl cleavage of α-ketoaldehyde, which was formed after dehydration of the opened form of glucuronic acid. Subsequent cyclisation and

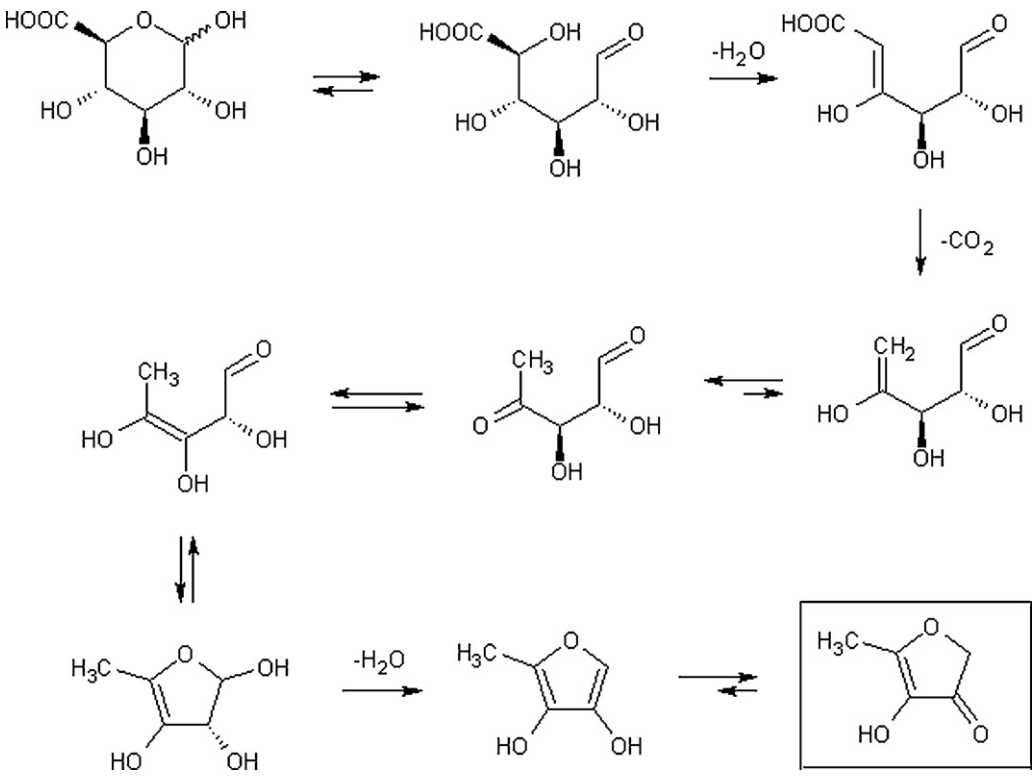

Fig. 5. Possible way of formation of 4-hydroxy-5-methyl-3-furanone during acid hydrolysis of hyaluronan.

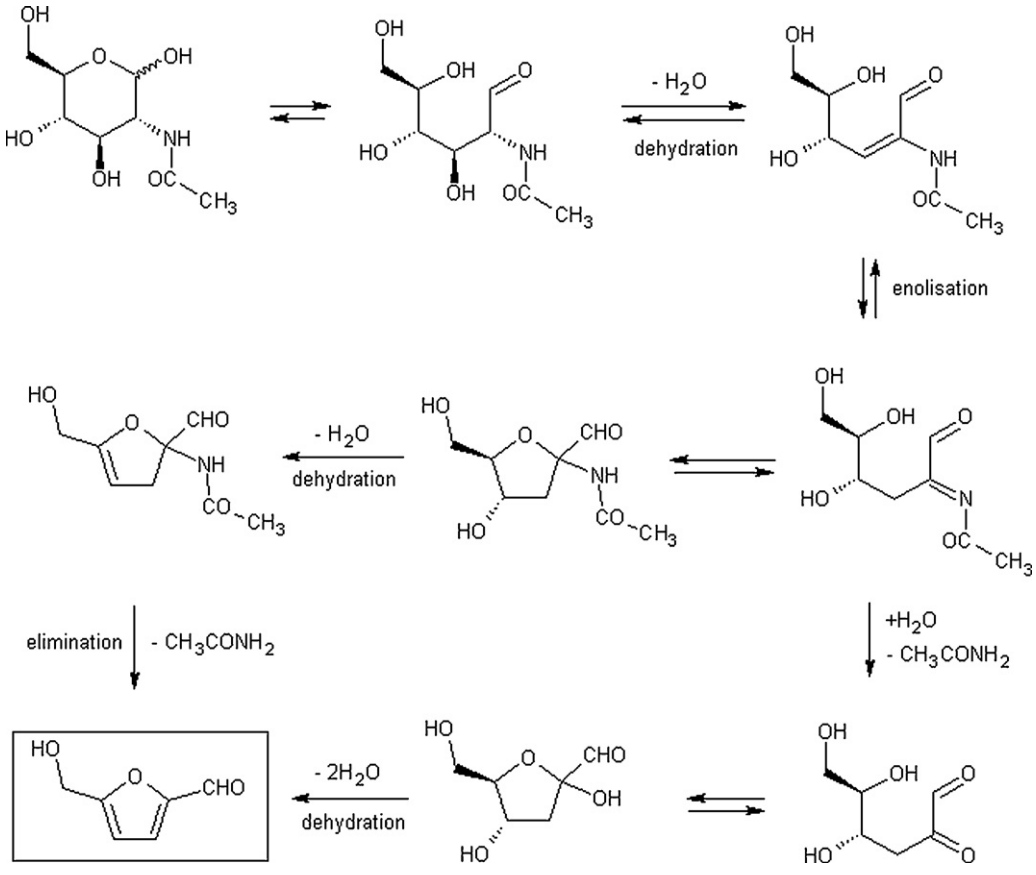

Fig. 6. Possible way of formation of 5-(hydroxymethyl)furfural during acid hydrolysis of hyaluronan.

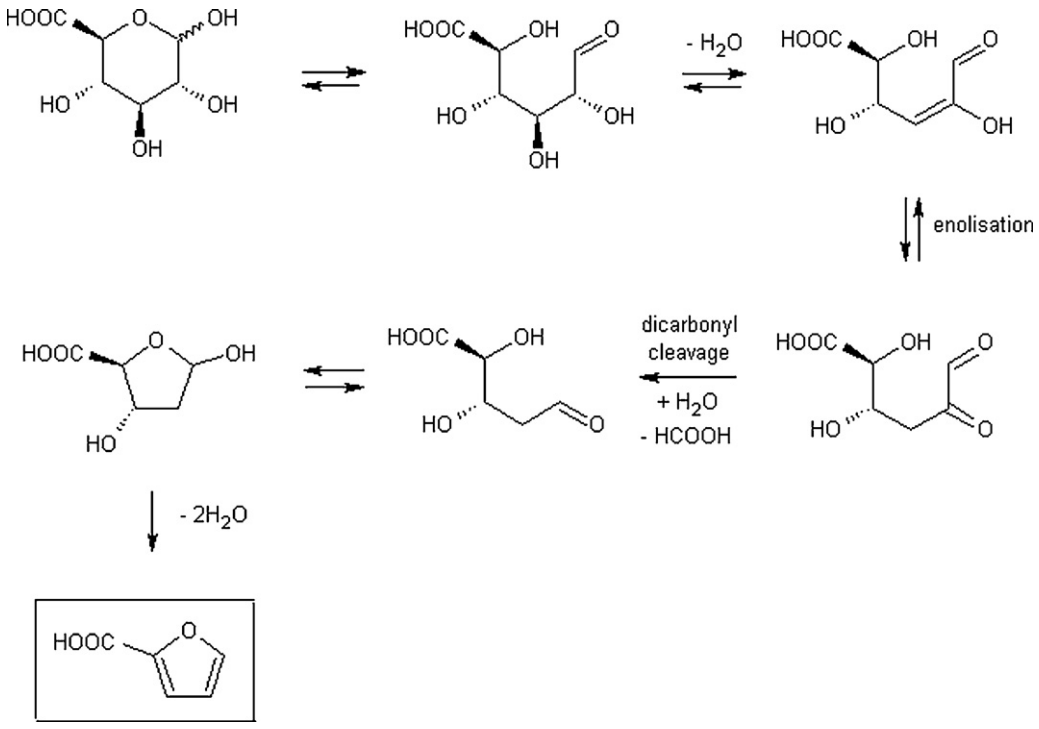

Fig. 7. Possible way of formation of 2-furoic acid during acid hydrolysis of hyaluronan.

irreversible double-dehydration yielded stable aromatic furane ring substituted with COOH group.

4. Conclusion

This work has demonstrated that a part of hyaluronan degradation products after acid hydrolysis is toxic and therefore, their amount in HA products prepared by acid hydrolysis should be always checked, when low molar mass hyaluronan is produced with the intention of cosmetic or pharmaceutical application. Since the degradation byproducts can be completely removed by ultrafiltration from the reaction mixture, the ultrafiltration step is recommended to be always used prior isolation of low molar mass hyaluronan.

References

Boisen, A., Christensen, T. B., Fu, W., Gorbanev, Y. Y., Hansen, T. S., Jensen, J. S., et al. (2009). Process integration for the conversion of glucose to 2,5-furandicarboxylic acid. *Chemical Engineering Research and Design*, *87*, 1318–1327.

Delmage, J. M., Powars, D. R., Jaynes, P. K., & Allerton, S. E. (1986). The selective suppression of immunogenicity by hyaluronic acid. *Annals of Clinical Laboratory Science*, *16*, 303–310.

Deschrevel, B., Tranchepain, F., & Vincent, J. (2008). Chain-length dependence of the kinetics of the hyaluronan hydrolysis catalyzed by bovine testicular hyaluronidase. *Matrix Biology*, *27*, 475–486.

Fitzgerald, K. A., Bowie, A. G., Skeffington, B. S., & O'Neill, L. A. (2000). Ras, protein kinase C zeta, and I kappa B kinases 1 and 2 are downstream effectors of CD44 during the activation of NF-kappa B by hyaluronic acid fragments in T-24 carcinoma cells. *Journal of Immunology*, *164*, 2053–2063.

Gandini, A., & Belgacem, M. N. (1997). Furans in polymer chemistry. *Progress in Polymer Science*, *22*, 1203–1379.

Gandini, A., & Belgacem, M. N. (2002). Recent contributions to the preparation of polymers derived from renewable resources. *Journal of Polymers and the Environment*, *10*, 105–114.

Kakumanu, V. K., Arora, V. K., & Bansal, A. K. (2006). Development and validation of isomer specific RP-HPLC method for quantification of cefpodoxime proxetil. *Journal of Chromatography B*, *835*, 16–20.

Kroh, L. W. (1994). Caramelisation in food and beverages. *Food Chemistry*, *51*, 373–379.

Lambert, J. B., & Mazzola, E. P. (2003). *Nuclear magnetic resonance spectroscopy*. New Jersey: Pearson Education Inc.

Laurent, T. C., & Fraser, J. R. (1992). Hyaluronan. *FASEB Journal*, *6*, 2397–2404.

Laurent, T. C., Laurent, U. B. G., & Fraser, J. R. (1995). Functions of hyaluronan. *Annals of the Rheumatic Diseases*, *54*, 429–432.

McKee, C. M., Lowenstein, C. J., horton, M. R., Wu, J., Bao, C., Chin, B. Y., et al. (1997). Hyaluronan fragments induce nitric-oxide synthase in murine macrophages through a nuclear factor NF-κB-dependent mechanism. *Journal of Biological Chemistry*, *272*, 8013–8018.

McKee, C. M., Penno, M. B., Cowman, M., Burdick, M. D., Strieter, R. M., Bao, C., et al. (1996). Hyaluronan (HA) fragments induce chemokine gene expression in alveolar macrophages. The role of HA size and CD 44. *Journal of Clinical Investigation*, *98*, 2403–2413.

Melander, C., & Tømmeras, K. (2010). Heterogeneous hydrolysis of hyaluronic acid in ethanolic HCl slurry. *Carbohydrate Polymers*, *82*, 874–879.

Moreaua, C., Belgacem, M. N., & Gandini, A. (2004). Recent catalytic advances in the chemistry of substituted furans from carbohydrates and in the ensuing polymers. *Topics in Catalysis*, *27*, 11–30.

Tokita, Y., & Okamoto, A. (1995). Hydrolytic degradation of hyaluronic acid. *Polymer Degradation and Stability*, *48*, 269–273.

Tong, X., Ma, Y., & Li, Y. (2010). Biomass into chemicals: conversion of sugars to furan derivatives by catalytic processes. *Applied Catalysis A: General*, *385*, 1–13.

Vistejnova, L., Dvorakova, J., Hasova, M., Muthny, T., Velebny, V., Soucek, K., et al. (2009). The comparison of impedance-based method of cell proliferation monitoring with commonly used metabolic-based techniques. *Neuroendocrinology Letters*, *30*, 121–127.